205 800

Columbia University
in the City of New York

DEPARTMENT OF CIVIL ENGINEERING
AND ENGINEERING MECHANICS

STRESSES IN A LINEAR INCOMPRESSIBLE VISCO-ELASTIC CYLINDER WITH ANNIHILATING INNER SURFACE

by

M. Shinozuka

Office of Naval Research
Project Nonr 064-446
Contract Nonr 266(78)
Technical Report No. 12
CU-12-62-ONR 266(78) CE

March 1962

Columbia University
in the City of New York

DEPARTMENT OF CIVIL ENGINEERING
AND ENGINEERING MECHANICS

STRESSES IN A LINEAR INCOMPRESSIBLE VISCO-ELASTIC CYLINDER WITH ANNIHILATING INNER SURFACE

by

M. Shinozuka

Office of Naval Research
Project Nonr 064-446
Contract Nonr 266(78)
Technical Report No. 12
CU-12-62-ONR 266(78) CE

March 1962

SUMMARY

A method is developed to find the stresses and strains in an incompressible visco-elastic hollow cylinder with annihilating inner radius contained by an elastic case and subject to internal pressure under the assumption of a state of plane strain.

Stresses and strains are computed for a material with deviatoric stress-strain relations characteristic of a standard solid. The numerical computation is carried out with the aid of an I.B.M. digital computer 1620 and is intended to illustrate the effects of the thickness of the cylinder, of the rate of increase of the internal pressure and of the strength of the reinforcement provided by the elastic shell.

TABLE OF CONTENTS

LIST OF ILLUSTRATIONS

1. Introduction

The problem of evaluation of stresses and strains in a solid propellant with a burning inner surface under internal pressure has not yet been solved in a general way because of the evident difficulty of the treatment of the boundary condition at the moving inner surface.

It is the purpose of the present investigation to find a solution of this problem by evaluating stresses and strains in an elastically case-bonded linear visco-elastic hollow cylinder with annihilating inner surface subject to internal pressure.

For simplicity, incompressibility of the material and a state of plain strain are assumed; hence

$$\varepsilon_r = e_r, \quad \varepsilon_\theta = e_\theta, \quad \varepsilon_z = e_z = 0$$

$$\varepsilon_r = du/dr, \quad \varepsilon_\theta = u/r$$

$$\varepsilon_r + \varepsilon_\theta = \frac{du}{dr} + \frac{u}{r} = 0 \tag{1}$$

where ε_r, ε_θ, e_r and e_θ are respectively the radial and tangential components of strain and deviatoric strain, and u is the radial displacement.

Eq. (1) is satisfied by $u = k(t)/r$ where $k(t)$ is a function of time t only. Hence,

$$\varepsilon_r = -k(t)/r^2, \quad \varepsilon_\theta = k(t)/r^2 \tag{2}$$

When s_{ij} and e_{ij} respectively denote the components of deviatoric stress and strain, the stress-strain relations for incompressible linear visco-elastic materials are of the well-known form

$$P(s_{ij}) = Q(e_{ij}) \tag{3}$$

where $\mathbb{P}$ and $\mathbb{Q}$ are linear differential operators with respect to time t or, in terms of Laplace transforms with initially zero condition,

$$\bar{\mathbb{P}}(p)\bar{s}_{ij}(p) = \bar{\mathbb{Q}}(p)\bar{e}_{ij}(p) \tag{3'}$$

where p denotes the transform parameter.

The equation of equilibrium

$$\frac{d\sigma_r}{dr} + \frac{\sigma_r - \sigma_\theta}{r} = 0 \quad or \quad \frac{d s_r}{dr} + \frac{s_r - s_\theta}{r} = 0 \tag{4}$$

when $\mathbb{P}$ operates on both sides with assumed interchangeability between differentiations with respect to time t and radius r becomes

$$\frac{d}{dr}\left\{\mathbb{P}(\sigma_r)\right\} = \left\{\mathbb{P}(s_\theta) - \mathbb{P}(s_r)\right\}/r = \left\{\mathbb{Q}(e_\theta) - \mathbb{Q}(e_r)\right\}/r$$

after the stress-strain relation Eq. (3) has been introduced.

Substituting Eq. (2) into the above equation gives

$$\frac{d}{dr}\left\{\mathbb{P}(\sigma_r)\right\} = \frac{2}{r^3}\mathbb{Q}\left\{k(t)\right\}$$

from which $\mathbb{P}(\sigma_r)$ is obtained by integration with respect to r:

$$\mathbb{P}(\sigma_r) = -\frac{1}{r^2}\mathbb{Q}\left\{k(t)\right\} + C(t) \tag{5}$$

where C(t) is a function of t only.

The equilibrium of the elastic shell requires the relation

$$\sigma_r]_{r=b} = -\frac{h}{b}\sigma_c$$

between the shell stress σ_c and the radial stress of the cylinder $\sigma_r]_{r=b}$ at the interface between the cylinder and the shell, while σ_c is in turn

related to the strain of the cylinder $\varepsilon_\theta]_{r=b}$ at this interface by the relation

$$\sigma_c = \frac{E_c}{1-\nu_c^2}\, \varepsilon_\theta]_{r=b}$$

since $\varepsilon_\theta]_{r=b}$ is identical to the shell strain ε_c; h is the thickness of the shell, b the outer radius of the hollow cylinder and E_c and ν_c are Young's modulus and Poisson ratio of the shell respectively.

Therefore the first boundary condition at r = b has the form

$$\sigma_r]_{r=b} = -E_c''\, \varepsilon_\theta]_{r=b} = -E_c'' \frac{k(t)}{b^2} \qquad (6)$$

or

$$\mathbb{P}(\sigma_r)]_{r=b} = -\frac{E_c''}{b^2}\mathbb{P}\{k(t)\} \qquad (6')$$

where the second of Eqs. (2) has been introduced for ε_θ, and

$$E_c'' = \frac{E_c}{1-\nu_c^2}\cdot\frac{h}{b}\ . \qquad (7)$$

C(t) is obtained from Eqs. (5) and (6'):

$$C(t) = \frac{1}{b^2}\mathbb{Q}\{k(t)\} - \frac{E_c''}{b^2}\mathbb{P}\{k(t)\}$$

Hence

$$\mathbb{P}(\sigma_r) = \left(\frac{1}{b^2}-\frac{1}{r^2}\right)\mathbb{Q}\{k(t)\} - \frac{E_c''}{b^2}\mathbb{P}\{k(t)\}\ . \qquad (8)$$

However, as pointed out by E. H. Lee, R. M. Radok and W. B. Woodward [1], it is not possible to operate with $\mathbb{P}$ on the second boundary condition at

the inner surface

$$-\sigma_r\big]_{r=a(t)} = p(t) \tag{9}$$

and substitute it into Eq. (5) as in the first boundary condition, since Eq. (5) is essentially a relation between stress and strain associated with a fixed material particle, while at each instant $\sigma_r]_{r=a(t)}$ in Eq. (9) represents the radial stress of a different material particle; $a(t)$ is a monotonically increasing function of time representing the inner radius of the hollow cylinder until

$$a(t_o) = b \tag{10}$$

is reached when the annihilation is completed at $t = t_o$.

2. <u>General Expressions for Stresses and Strains</u>

The difficulty is removed however if the stress-strain relation is expressed in the form

$$s_{ij} = \mathcal{L}(e_{ij}) \tag{11}$$

instead of Eq. (3), where $\mathcal{L}$ is a linear operator in derivatives and integrals with respect to time only, or in terms of its Laplace transform under zero initial conditions:

$$\bar{s}_{ij}(p) = \bar{\mathcal{L}}(p)\bar{e}_{ij}(p) \tag{11'}$$

The substitution of Eq. (2) into Eq. (11) gives

$$s_r = -\frac{1}{r^2}\mathcal{L}\left\{k(t)\right\}, \quad s_\theta = \frac{1}{r^2}\mathcal{L}\left\{k(t)\right\}$$

The radial stress σ_r is then obtained from Eq. (4):

$$\sigma_r = -\frac{1}{r^2}\mathcal{L}\{k(t)\} + D(t)$$

where D(t) is a function of t only.

Use of the first boundary condition Eq. (6) determines D(t):

$$D(t) = \frac{1}{b^2}\mathcal{L}\{k(t)\} - E_c'' \frac{k(t)}{b^2}$$

Hence

$$\sigma_r = \left(\frac{1}{b^2} - \frac{1}{r^2}\right)\mathcal{L}\{k(t)\} - E_c'' \frac{k(t)}{b^2} \tag{12}$$

The unknown function k(t) is now obtained from the integro-differential equation

$$-p(t) = \left(\frac{1}{b^2} - \frac{1}{a^2(t)}\right)\mathcal{L}\{k(t)\} - \frac{E_c''}{b^2}k(t) \tag{13}$$

which is the result of the application of the second boundary condition Eq. (9) to Eq. (12).

E. H. Lee, R. M. Radok and W. B. Woodward [1] solved a special case of the problem in which the mechanical model of the material was assumed to be a Kelvin body. This implies a stress-strain relation of the form Eq. (11) with

$$\mathcal{L} = 2G + 2\eta\frac{\partial}{\partial t}$$

or of the form of Eq. (11') with

$$\bar{\mathcal{L}}(p) = 2G + 2\eta p;$$

G denotes the shear modulus and η the coefficient of viscosity in shear as shown in Fig. 1.

In more generality linear visco-elastic material can be represented [2]

by n Maxwell elements coupled in parallel with discrete relaxation times $\tau_i = \eta_i/G_i$ (Fig. 2) and normalized discrete relaxation spectrum $F_i(\tau_i) = G_i(\tau_i)/G$ (Fig. 3) or by the limit of the same model when n approaches infinity with continuous relaxation time τ and normalized continuous relaxation spectrum $f(\tau) = g(\tau)/G$ where the unrelaxed shear modulus $G = \sum_{i=1}^{n} G_i$ or $G = \int_0^{\infty} g(\tau)d\tau$. It can then be shown [3] that the stress deviation is related to the strain deviation in the form

$$s_{ij} = 2G\left[e_{ij} + \int_0^t \dot{\psi}(t-\theta)\, e(\theta)\, d\theta\right] \tag{14}$$

or in the form of Eq. (11') with

$$2\bar{\mathcal{L}}(p) = 2G\left\{1 + \bar{\dot{\psi}}(p)\right\} .$$

The relaxation-rate-function $\dot{\psi}(t) = d\psi(t)/dt$ (this notation for the time derivative is used henceforth) in Eq. (14) is the time derivative of the relaxation-function $\psi(t)$ which is defined so as to produce the stress response to the unit step strain input $e_{ij}(t) = e_o = \text{const.}$ in the form $s_{ij}(t) = 2Ge_o\psi(t)$. $\psi(t)$ can also be obtained from a knowledge of the relaxation spectrum:

$$\dot{\psi}(t) = -\sum_{i=1}^{n} \frac{F_i}{\tau_i} e^{-t/\tau_i} \tag{15}$$

for the discrete relaxation spectrum and

$$\dot{\psi}(t) = -\int_0^{\infty} \frac{f(\tau)}{\tau} e^{-t/\tau}\, d\tau \tag{16}$$

for the continuous relaxation spectrum. Eq. (12) can now be written in the form

$$\sigma_r = 2G\left(\frac{1}{b^2} - \frac{1}{r^2}\right)\left[k(t) + \int_0^t \dot{\psi}(t-\theta)\, k(\theta)\, d\theta\right] - \frac{E_2''}{b^2} k(t) \tag{12'}$$

The determining equation Eq. (13) for k(t) then becomes

$$-p(t) = 2G\left(\frac{1}{b^2} - \frac{1}{a^2(t)}\right)\left[k(t) + \int_0^t \dot{\psi}(t-\theta)k(\theta)\,d\theta\right] - \frac{E_c''}{b^2}k(t) \tag{13'}$$

which can be reduced to the form of Volterra's integral equation:

$$k(t) + \frac{\frac{1}{a^2(t)} - \frac{1}{b^2}}{\frac{1}{a^2(t)} + \frac{\mu - 1}{b^2}} \int_0^t \dot{\psi}(t-\theta)k(\theta)\,d\theta = \frac{p(t)}{2G\left(\frac{1}{a^2(t)} + \frac{\mu - 1}{b^2}\right)} \tag{17}$$

where $\mu = E_c''/2G$.

The solution k(t) of Eq. (17) furnishes the strains with the aid of Eq. (2). The radial stress σ_r is obtained from Eq. (12'), which involves the integration of k(t). However, the identity from Eq. (13')

$$2G\left[k(t) + \int_0^t \dot{\psi}(t-\theta)k(\theta)\,d\theta\right] = \left\{\frac{E_c''}{b^2}k(t) - p(t)\right\} \Big/ \left(\frac{1}{b^2} - \frac{1}{a^2(t)}\right) \tag{18}$$

can be used to avoid the evaluation of this integral writing the radial stress σ_r in the form

$$\sigma_r = \frac{\frac{1}{b^2} - \frac{1}{r^2}}{\frac{1}{b^2} - \frac{1}{a^2(t)}}\left[\frac{E_c''}{b^2}k(t) - p(t)\right] - \frac{E_c''}{b^2}k(t) \qquad (t \neq t_0) \tag{19}$$

The tangential stress σ_θ is obtained from the equation of equilibrium Eq. (4):

$$\sigma_\theta = \frac{\frac{1}{b^2} + \frac{1}{r^2}}{\frac{1}{b^2} - \frac{1}{a^2(t)}}\left[E_c''\frac{k(t)}{b^2} - p(t)\right] - E_c''\frac{k(t)}{b^2} \qquad (t \neq t_0). \tag{20}$$

when t approaches t_o, the right hand side of Eq. (18) should be interpreted as the limit:

$$q(t_o) = 2G\left[k(t_o) + \int_0^{t_o} \psi(t_o - \theta) k(\theta)\, d\theta\right] = \lim_{t \to t_o} \frac{E_c'' \frac{k(t)}{b^2} - p(t)}{\frac{1}{b^2} - \frac{1}{a^2(t)}} \tag{21}$$

since $\lim_{t \to t_o} a(t) = b$ from Eq. (10) and $\lim_{t \to t_o} E_c'' \frac{k(t)}{b^2} = \lim_{t \to t_o} p(t)$ from Eq. (13'). Hence, as t approaches t_o, the stresses are given by

$$\sigma_r = -p(t_o) \tag{22}$$

$$\sigma_\theta = \frac{2}{b^2} q(t_o) - p(t_o) \tag{23}$$

since $\lim_{t \to t_o} r = b$.

3. <u>Stresses and Strains for Medium with Standard Solid Stress-Strain Relation</u>

When the stress-strain relation in shear is represented by a standard solid (Fig. 4), the relaxation time τ_1 is considered infinite while $\tau_2 = \eta_2/G_2$. The relaxation-rate-function $\dot{\psi}(t)$ is obtained from Eq. (15)

$$\dot{\psi}(t) = -\frac{1-\alpha}{\tau_2} e^{-t/\tau_2} \tag{15'}$$

where $\alpha = F_1 = G_1/(G_1 + G_2)$

The substitution of Eq. (15') into Eq. (17) produces

$$h(t) - \frac{1-\alpha}{\tau_2} \cdot \frac{\frac{1}{a^2(t)} - \frac{1}{b^2}}{\frac{1}{a^2(t)} + \frac{\mu - 1}{b^2}} \int_0^t h(\theta)\, d\theta = \frac{p(t) e^{t/\tau_2}}{2G\left(\frac{1}{a^2(t)} + \frac{\mu - 1}{b^2}\right)} \tag{17'}$$

where $h(t) = k(t)e^{t/\tau_2}$.

Both sides of Eq. (17') are now divided by the coefficient of the integral on the left hand side and differentiated once with respect to time so as to produce the differential equation

$$f(t)\dot{h}(t) + [\dot{f}(t) - 1]\, h(t) = \dot{g}(t) \tag{24}$$

where

$$f(t) = \frac{\tau_2}{1-\alpha} \cdot \frac{\frac{1}{a^2(t)} + \frac{\mu - 1}{b^2}}{\frac{1}{a^2(t)} - \frac{1}{b^2}} \tag{25}$$

and

$$g(t) = \frac{\tau_2}{1-\alpha} \cdot \frac{p(t)e^{t/\tau_2}}{2G\left(\frac{1}{a^2(t)} - \frac{1}{b^2}\right)} \ . \tag{26}$$

With an integrating factor $\exp\left[-\int_0^t \frac{d\tau}{f(\tau)}\right]$, Eq. (24) can be integrated:

$$h(t) = g(t)/f(t) + \frac{e^{\int_0^t \frac{d\tau}{f(\tau)}}}{f(t)} \int_0^t \frac{g(\tau)}{f(\tau)}\, e^{-\int_0^\tau \frac{dx}{f(x)}}\, d\tau$$

and therefore

$$k(t) = g(t)e^{-t/\tau_2}/f(t) + \frac{e^{-t/\tau_2}}{f(t)} e^{\int_0^t \frac{d\tau}{f(\tau)}} \int_0^t \frac{g(\tau)}{f(\tau)}\, e^{-\int_0^\tau \frac{dx}{f(x)}}\, d\tau \tag{27}$$

It is assumed that the annihilating rate of the inner surface is governed by the relation

$$a(t) = a_0\sqrt{1 - Kt} \tag{28}$$

with

$$\mathcal{K} = \frac{\rho_o^2 - 1}{\rho_o^2} \cdot \frac{1}{t_o} \tag{29}$$

where a_o is the initial inner radius (at $t = 0$) and $\rho_o = b/a_o$. $a(t)$ is plotted against t/t_o in Fig. 5 with ρ_o (= 1.5, 2.0 and 3) as parameter.

With the form of $a(t)$ given in Eq. (28), the integral $\int_0^t \frac{d\tau}{f(\tau)}$ can be evaluated so that

$$e^{\pm\int_0^t \frac{d\tau}{f(\tau)}} = e^{\pm\frac{1-\alpha}{\tau_2}t}\left(1 - \frac{B}{A}t\right)^{\pm\frac{1-\alpha}{\tau_2}\cdot\frac{A-A'}{B}}$$

where

$$A = \frac{1}{a^2(t)} + \frac{\mu - 1}{b^2}, \quad A' = \frac{1}{a^2(t)} - \frac{1}{b^2} \quad \text{and} \quad B = \frac{\mathcal{K}}{a_o^2}.$$

If the internal pressure $p(t)$ is assumed to be of the form

$$p(t) = p_o\left(1 - e^{-t/\tau_o}\right) \tag{30}$$

Eq. (27) becomes

$$k(t) = \frac{p_o\left(1 - e^{-t/\tau_o}\right)}{2G(A - Bt)} + \frac{p_o}{2G}\frac{A'}{A^2}\left(1 - \frac{B}{A}t\right)\left(1 - \frac{B}{A}\right)^{\gamma-1} e^{-\alpha t/\tau_2}\int_0^t \frac{\left(1 - e^{-\tau/\tau_o}\right)e^{\alpha\tau/\tau_2}}{\frac{\tau_2}{1-\alpha}\left(1 - \frac{B}{A}\tau\right)^{\gamma+1}}\, d\tau$$

which can be transformed by introducing the non-dimensional quantities $\sigma = p_o/(2G)$, $\alpha' = \tau_2/\tau_o$ and $\lambda = t_o/\tau_2$ into

$$\frac{k(t)}{b^2} = \frac{\sigma\zeta\left(1 - e^{-\alpha'\lambda\frac{t}{t_o}}\right)}{(\rho_o^2 - 1)\left(1 - \zeta\frac{t}{t_o}\right)} + \frac{\sigma\gamma^2\left(1 - \frac{t}{t_o}\right)\left(1 - \zeta\frac{t}{t_o}\right)^{\gamma-1}}{\rho_o^2 - 1}\, e^{-\alpha\lambda\frac{t}{t_o}}\varphi(t) \tag{31}$$

with

$$\varphi(t) = \int_0^{\frac{t}{t_o}} \frac{\lambda(1-\alpha)\left(1 - e^{-\alpha'\lambda T}\right)}{(1 - \zeta T)^{\gamma+1}}\, e^{\alpha\lambda T}\, dT \tag{32}$$

where

$$\xi = \frac{\lambda(1-\alpha)}{\gamma + \lambda(1-\alpha)} \text{ and } \gamma = \frac{(1-\alpha)}{\tau_2}\frac{(A-A')}{B} = \frac{\lambda(1-\alpha)\mu}{\rho_o^2 - 1} .$$

The integral $\varphi(t)$ can be numerically evaluated. The strains are

$$\varepsilon_r = -\frac{\rho_o^2}{R^2} \cdot \frac{k(t)}{b^2}, \quad \varepsilon_\theta = \frac{\rho_o^2}{R^2} \cdot \frac{k(t)}{b^2} \tag{33}$$

where $R = r/a_o$, while the stresses

$$\left.\begin{array}{l} \sigma_r/p_o \\ \sigma_\theta/p_o \end{array}\right\} = -\frac{1 \mp \rho_o^2/R^2}{(\rho_o^2-1)(1-\frac{t}{t_o})}\left[\frac{\gamma(\rho_o^2-1)}{\sigma(1-\alpha)\lambda} \cdot \frac{k(t)}{b^2} - (1 - e^{-\alpha'\lambda\frac{t}{t_o}})\right] - \frac{\gamma(\rho_o^2-1)}{\sigma(1-\alpha)\lambda} \cdot \frac{k(t)}{b^2} \tag{34}$$

$(t \neq t_o)$

$$\left.\begin{array}{l} \sigma_r/p_o = -(1 - e^{-\alpha'\lambda}) \\ \sigma_\theta/p_o = (\frac{2}{\mu} - 1)(1 - e^{-\alpha'\lambda}) - \frac{2\xi(1-\xi)^\gamma}{\rho_o^2 - 1} e^{-\alpha\lambda}\varphi(t_o) \qquad (t = t_o) \end{array}\right\} \tag{35}$$

Eq. (35) has been obtained considering that by l'Hospital's rule

$$q(t_o) = b^2 p_o \left[\frac{1}{\mu}(1 - e^{-\alpha'\lambda}) - \frac{\xi(1-\xi)^\gamma}{\rho_o^2 - 1} e^{-\alpha\lambda}\varphi(t_o)\right] .$$

4. Numerical Example

The previously defined non-dimensional quantities which characterize the problem are reviewed:

$\rho_o = b/a_o$ represents the original thickness of the cylinder.

$\lambda = t_o/\tau_2$ shows how much time is required for the total annihilation in terms of the relaxation time of the material.

$\alpha' = \tau_2/\tau_o$ is a measure of the build-up of internal pressure compared to the relaxation time of the material.

$\lambda\alpha' = t_o/\tau_o$ therefore indicates how rapidly the internal pressure is built up to the maximum in comparison with the total annihilation time t_o.

$\alpha = G_1/(G_1 + G_2)$ is related to the stress relaxation of the standard solid material in such a way that the permanent stress after completion of the stress relaxation under constant strain e_o is $s_\infty = 2Ge_o\alpha$ while the initial stress is $s_o = 2Ge_o$.

$\sigma = p_o/2G$ relates the magnitude of the maximum internal pressure to the unrelaxed shear modulus of the material.

$\mu = \frac{E_c''}{2G} = \frac{2G_c}{2G(1 - \nu_c)} \cdot \frac{h}{b}$ indicates the strength of the reinforcement due to the elastic shell where G_c and ν_c are the shear modulus and Poisson ratio of the elastic shell respectively.

The assignment of numerical values for these quantities is listed in Table 1 producing six different cases for which the numerical computations have been carried out using a 1620 I.B.M. digital computer.

Cases I-III are for comparison of the effect of the original thickness of the cylinder. The comparison of Cases I, IV and V shows the effect of either the rate of the application of the internal pressure when t_o is identical in these three cases (since then τ_o in Eq. (30) is equal to $t_o/10$, $t_o/5$ and t_o respectively) or the time t_o of total annihilation of the cylinder when $\tau_o = \tau_2$ is identical (since then $t_o = 10\tau_o$, $5\tau_o$ and τ_o respectively).

Finally Cases I and VI illustrate the reinforcing action of the elastic shell. In the latter the elastic shell is so strong that it gives rise to negative tangential stresses in the cylinder. Figs. 6(a), (b) and (c) respectively show the effect of the original thickness of the cylinder, the rate of the load application and of the rigidity of the elastic shell on the radial stress σ_r while Figs. 7 and 8 show these effects on the tangential stress and strain respectively. Fig. 9 shows the shell stresses σ_c/p_o with $h/b = 100$ for the six cases as functions of time t/t_o. Finally the space distributions of the radial stress for these six cases are also plotted at various times t/t_o in Fig. 10, while in Figs. 11 and 12 the space distributions of the tangential stress and strain are shown. In Figs. 10-12, vertical straight lines correspond to the positions of the inner surface at the specified time.

TABLE 1

Designation	ρ_o	λ	μ	
I	1.5	10	.5	$\alpha = .5$
II	2	10	.5	$\alpha' = 1.0$
III	3	10	.5	$\sigma = .1$
IV	1.5	5	.5	for all cases
V	1.5	1	.5	
VI	1.5	10	4	

References

[1] Lee, E. H., Radok, J. R. M. and Woodward, W. B., "Stress Analysis for Linear Viscoelastic Materials", Transactions of the Society of Rheology, Vol. III, Interscience Publishers, New York, 1959.

[2] Freudenthal, A. M. and Geiringer, H., "The Mathematical Theories of the Inelastic Continuum", Encyclopedia of Physics (Handbuch der Physik), Vol. VI, Springer-Verlag, Berlin, 1958, p. 273.

[3] Ibid. p. 274.

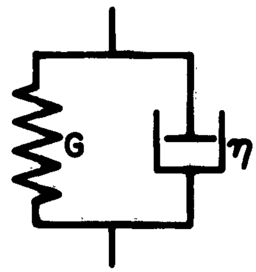

Figure 1. Kelvin Model

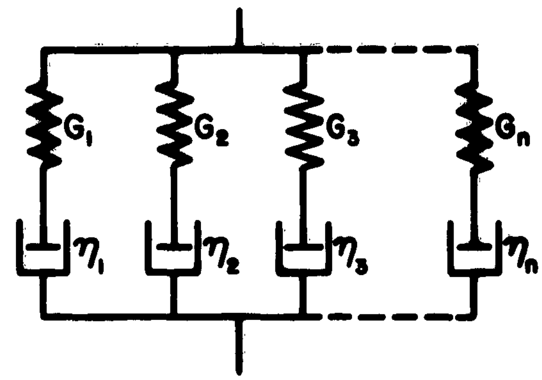

Figure 2. Maxwell Models Coupled in Parallel

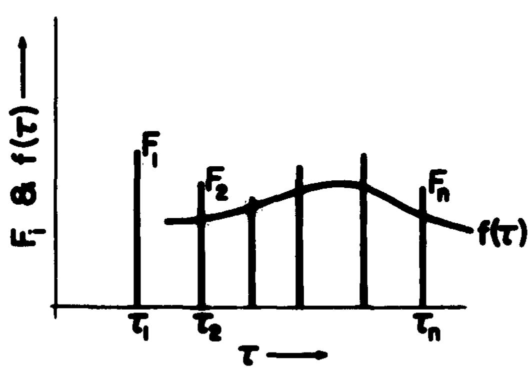

Figure 3. Relaxation Spectrum

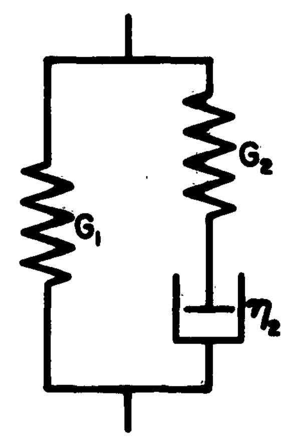

Figure 4. Standard Solid Model

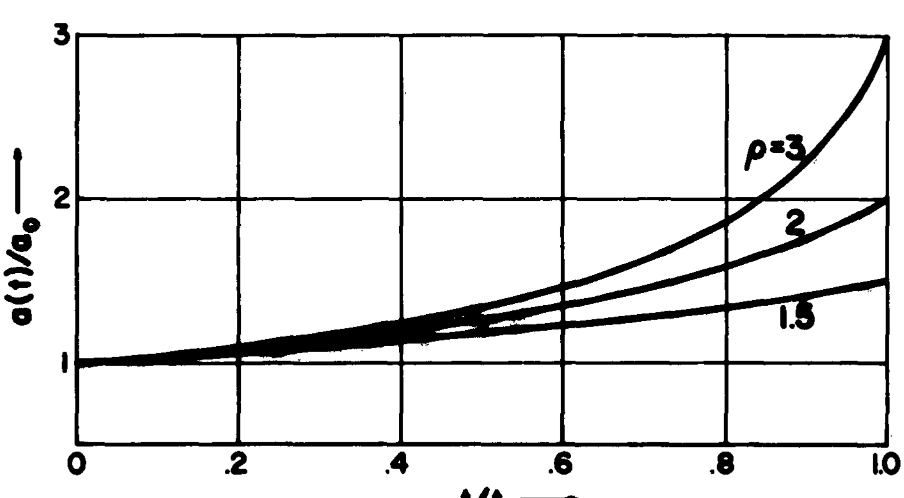

Figure 5. Annihilation of Inner Surface $a(t)/a_o$ as a Function of Time t/t_o

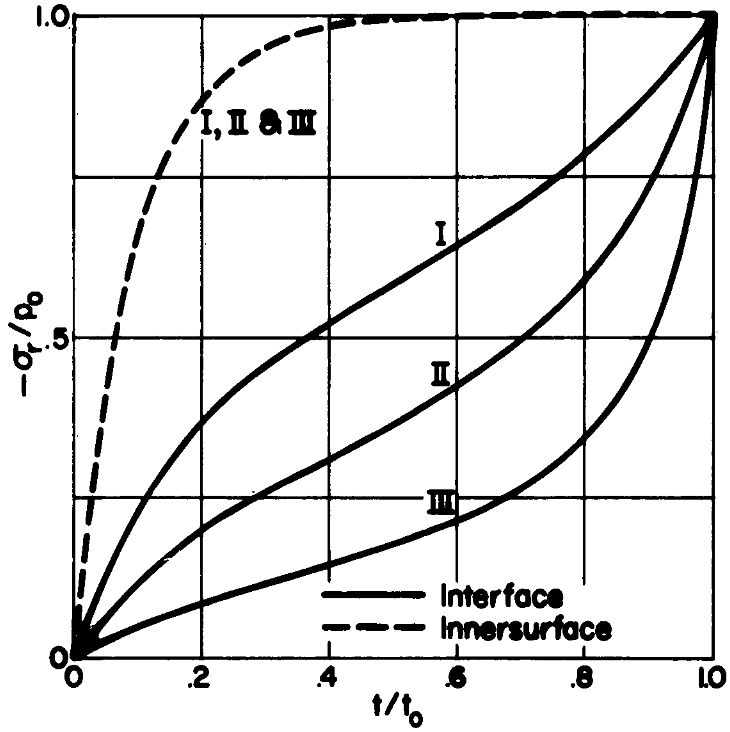

(a)

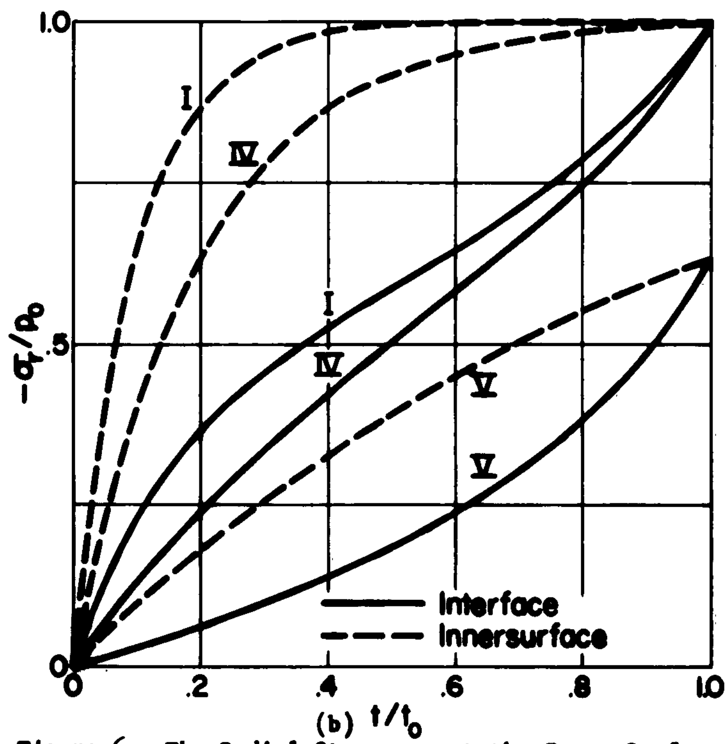

(b)

Figure 6. The Radial Stress σ_r at the Inner Surface and the Interface as a Function of Time t/t_o

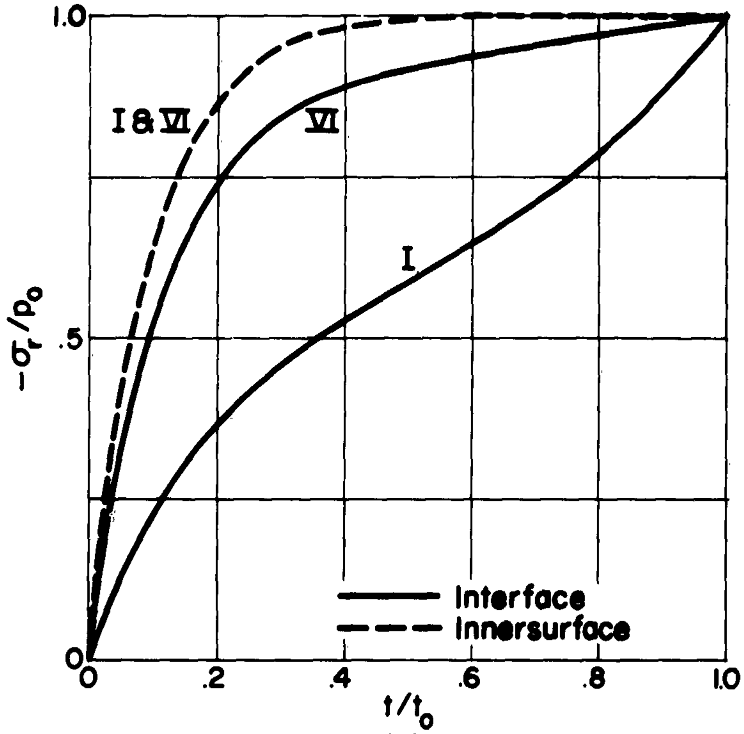

(c)

Figure 6. The Radial Stress σ_r at the Inner Surface and the Interface as a Function of Time t/t_o

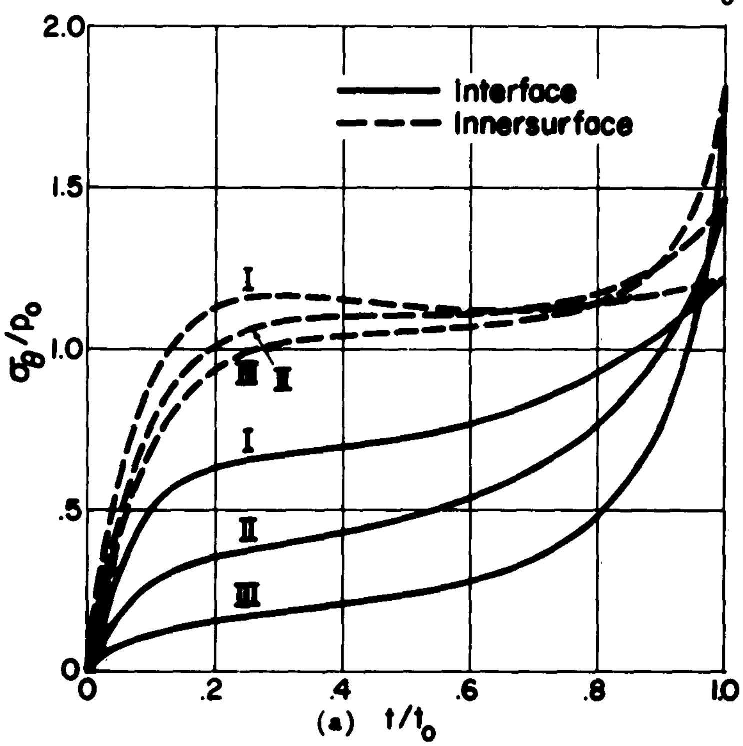

(a) t/t_o

Figure 7. The Tangential Stress σ_θ at the Inner Surface and the Interface as a Function of Time t/t_o

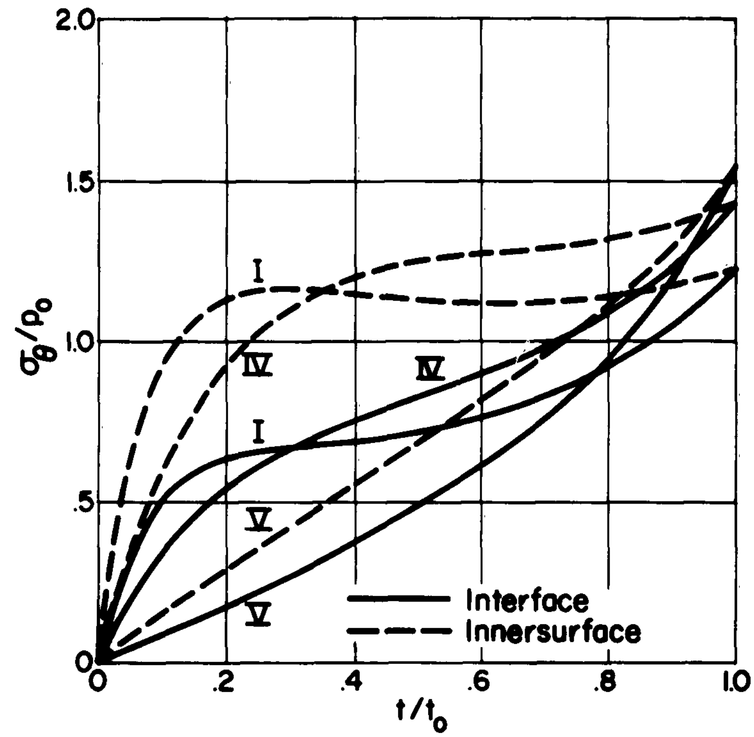

(b)

Figure 7. The Tangential Stress σ_{θ} at the Inner Surface and the Interface as a Function of Time t/t_o

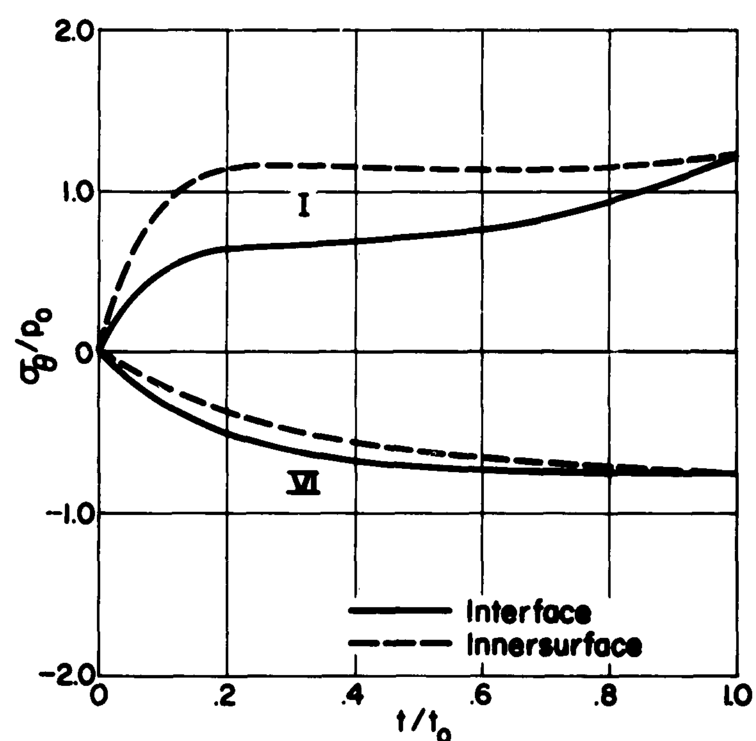

(c)

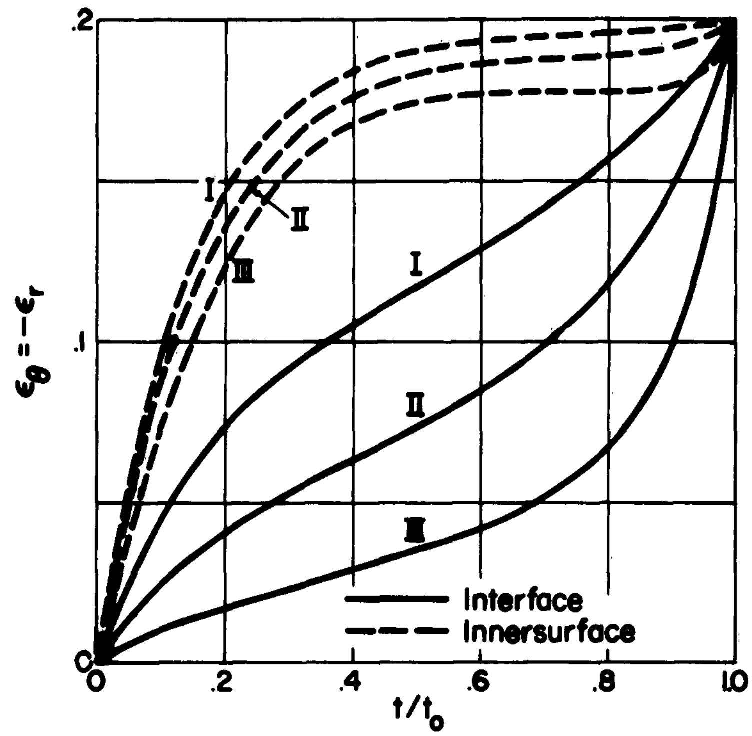

(a)

Figure 8. The Radial and Tangential Strains, ε_r and ε_θ, at the Inner Surface and Interface as Functions of Time t/t_o

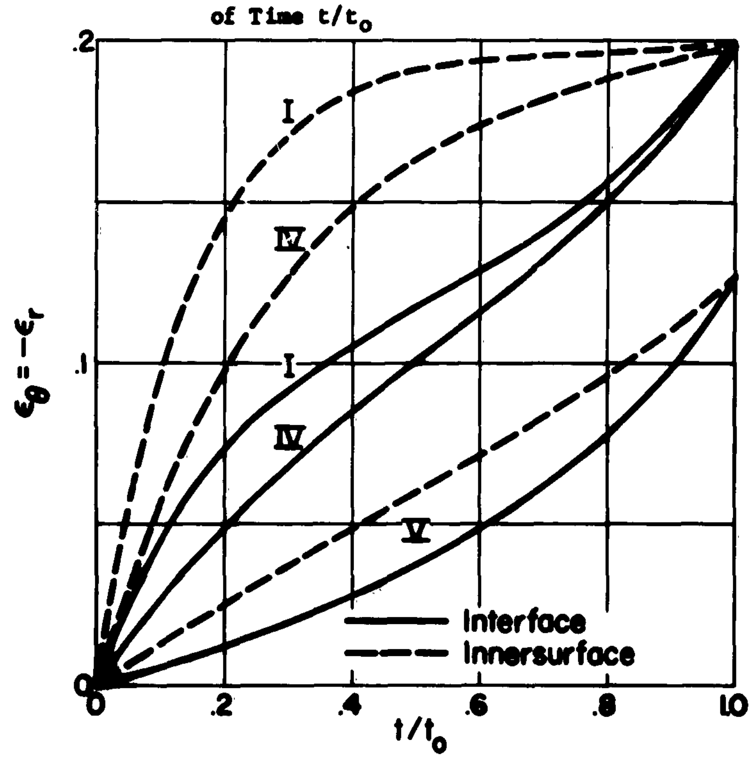

(b)

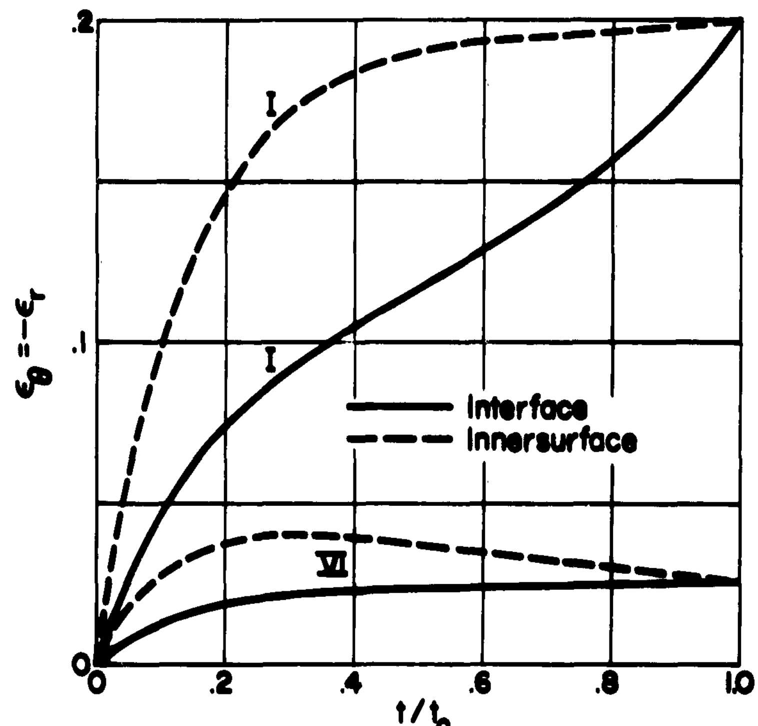

(c)

Figure 8. The Radial and Tangential Strains, ϵ_r and ϵ_θ, at the Inner Surface and the Interface as Functions of Time t/t_o

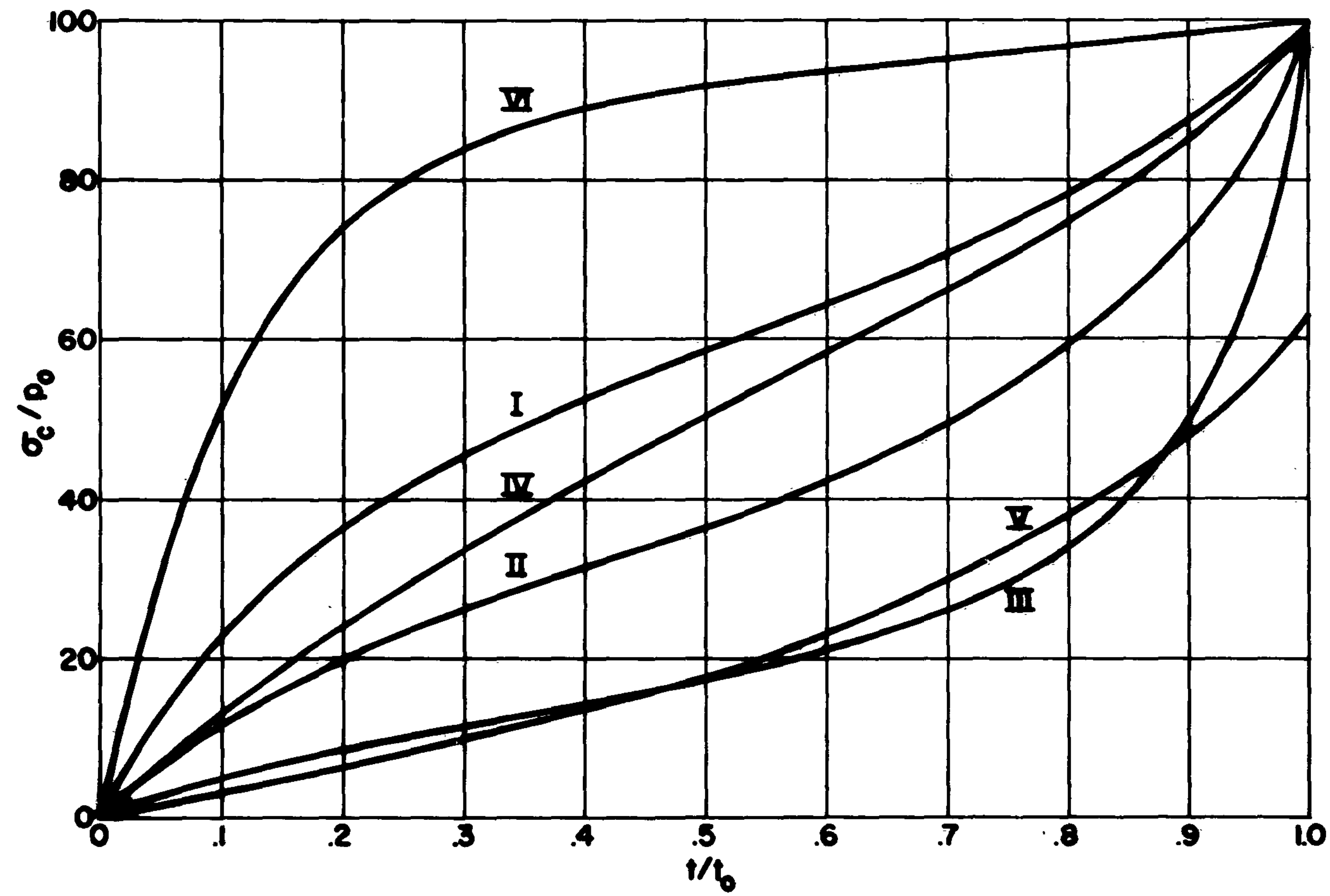

Figure 9. The Shell Stress σ_c as a Function of Time t/t_o

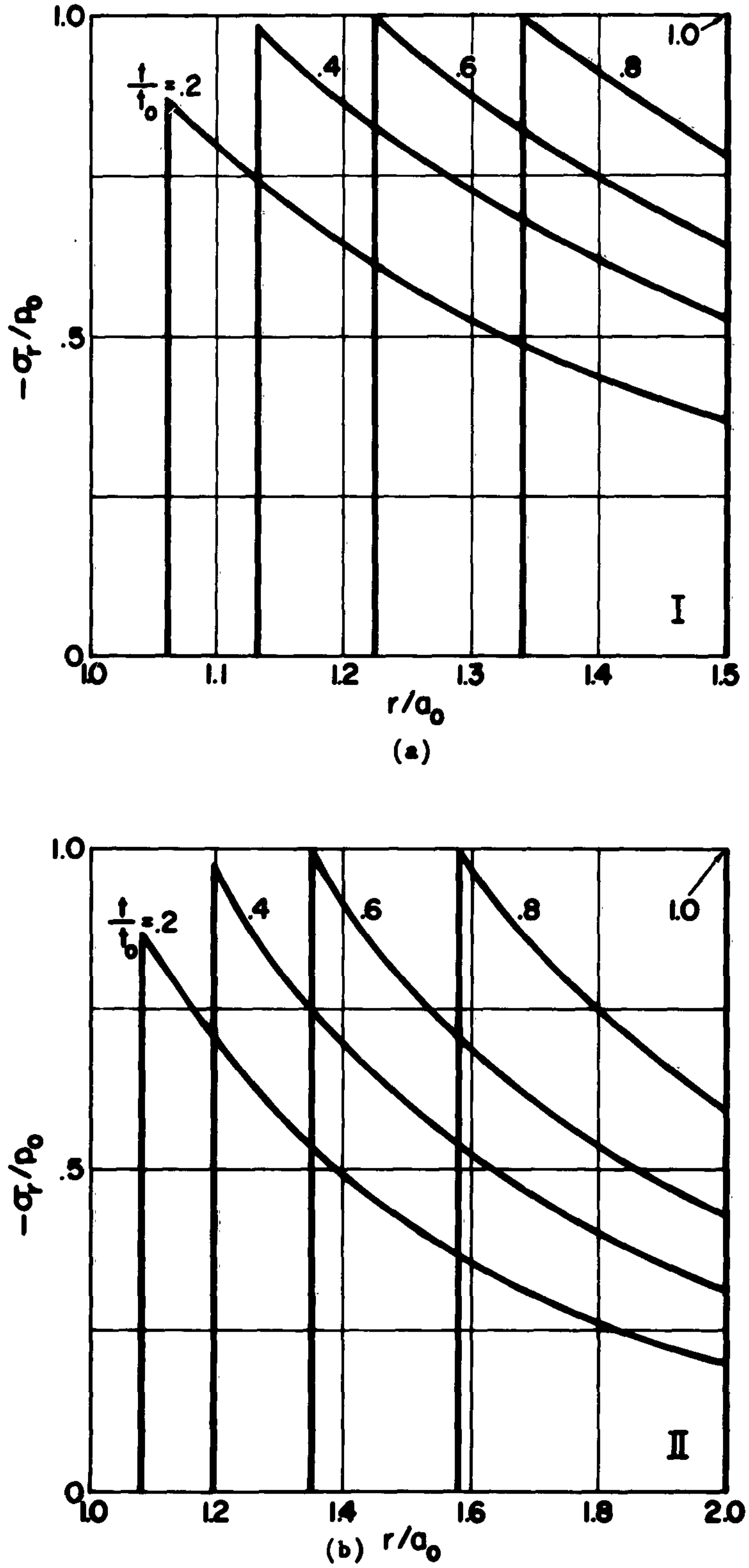

Figure 10. Space Distribution of Radial Stresses σ_r

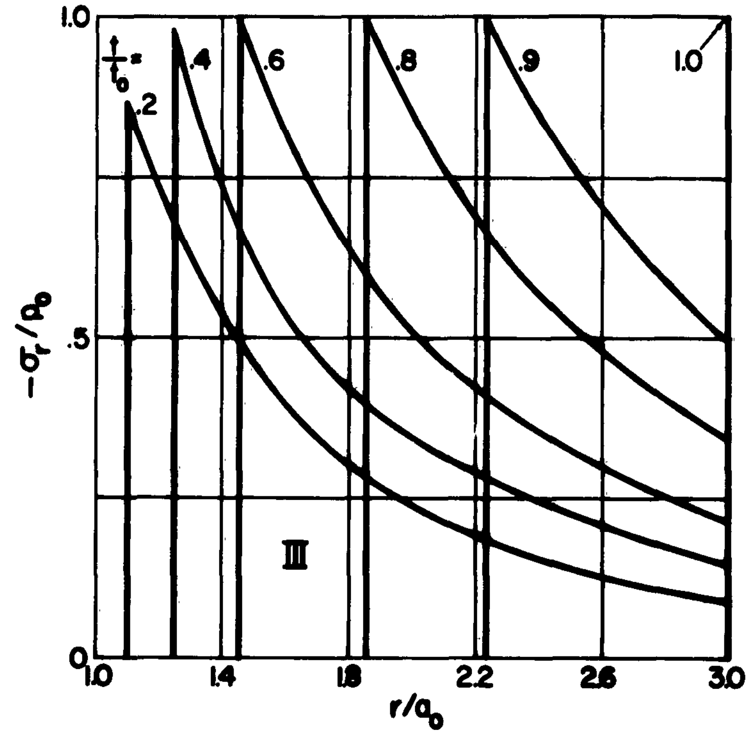

(c)

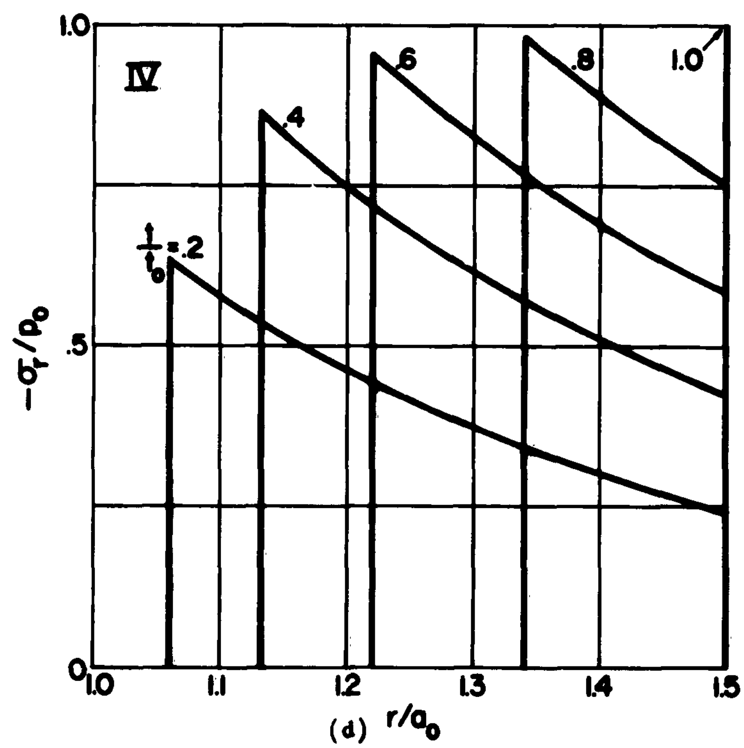

(d)

Figure 10. Space Distribution of Radial Stresses σ_r

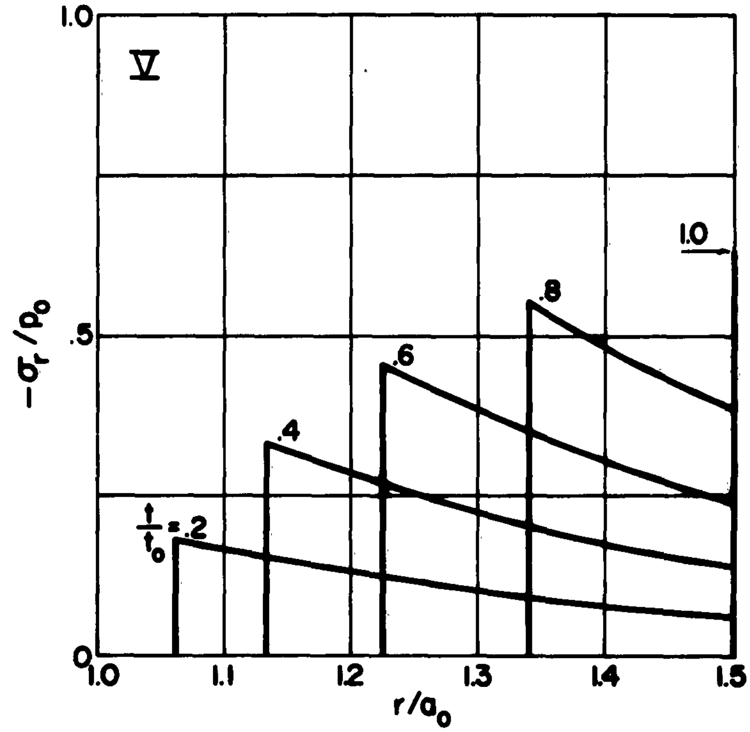

(e)

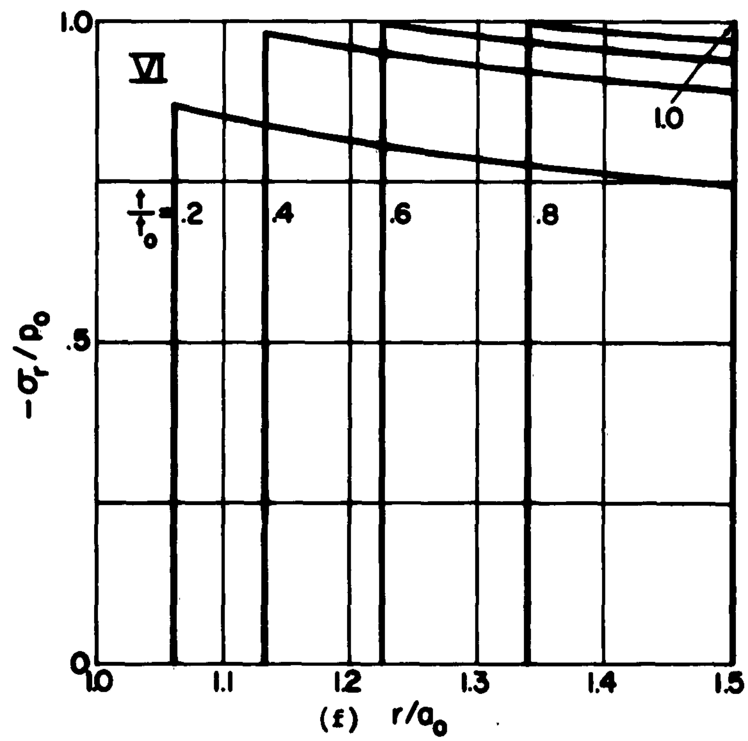

(f)

Figure 10. Space Distribution of Radial Stresses σ_r

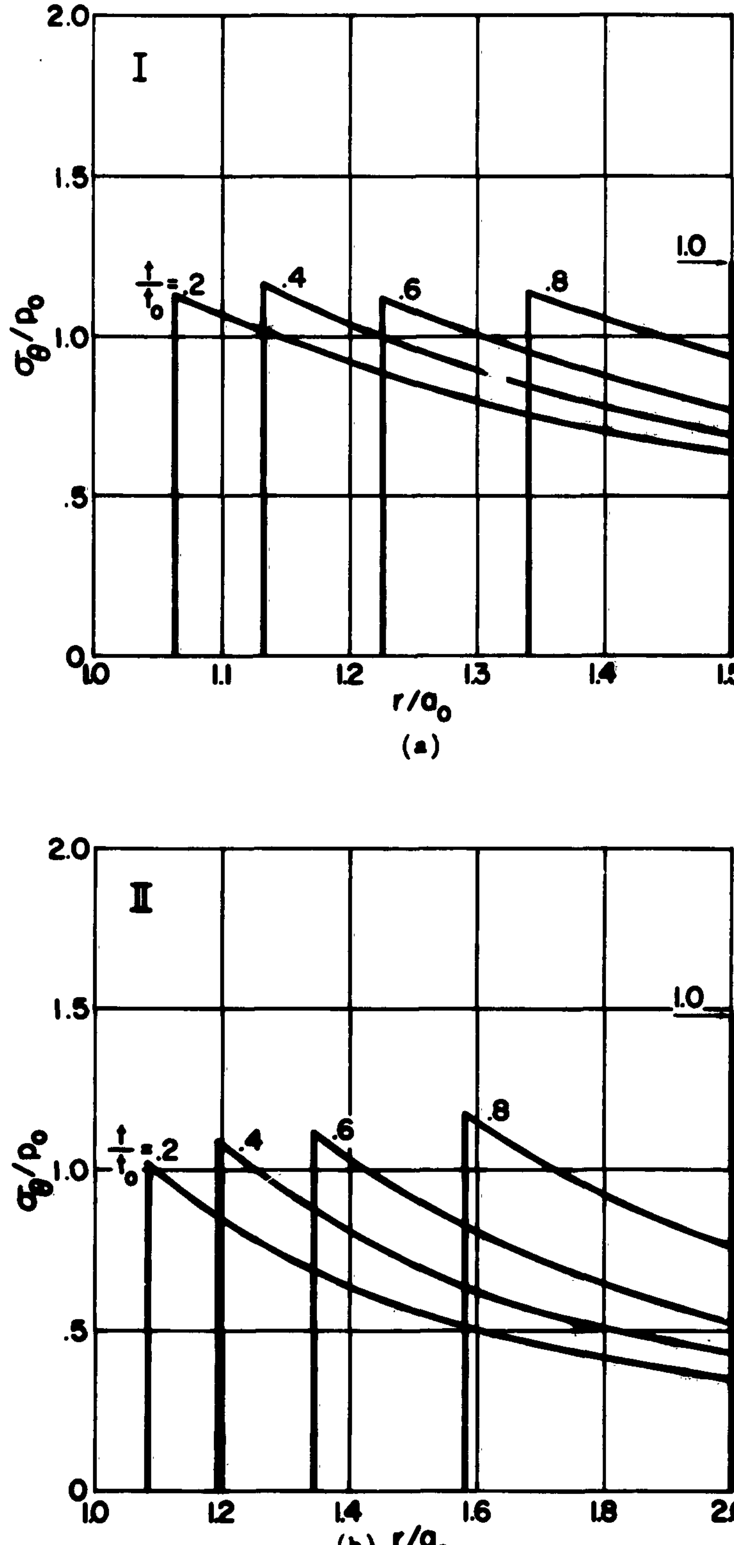

Figure 11. Space Distribution of Tangential Stresses σ_θ

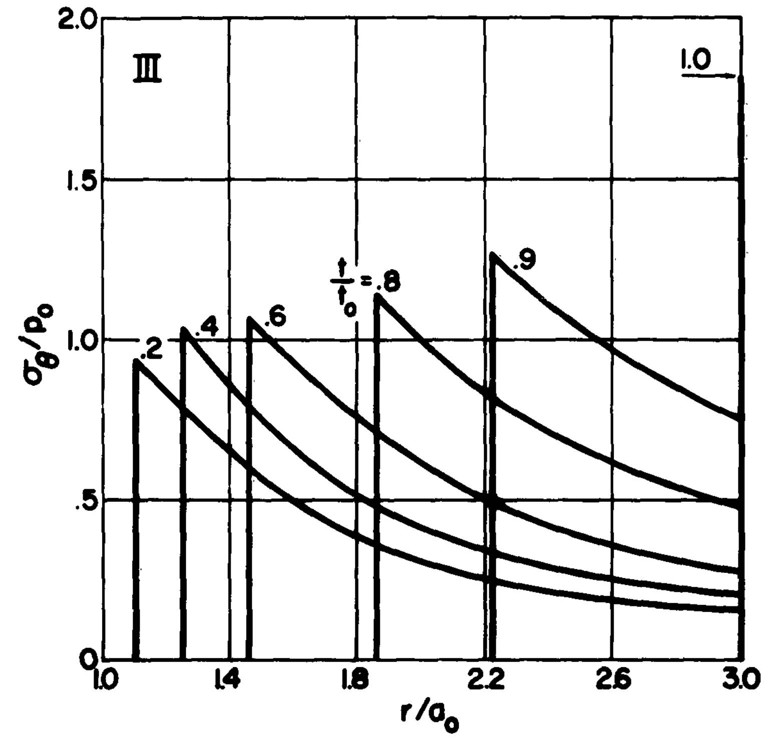

(c)

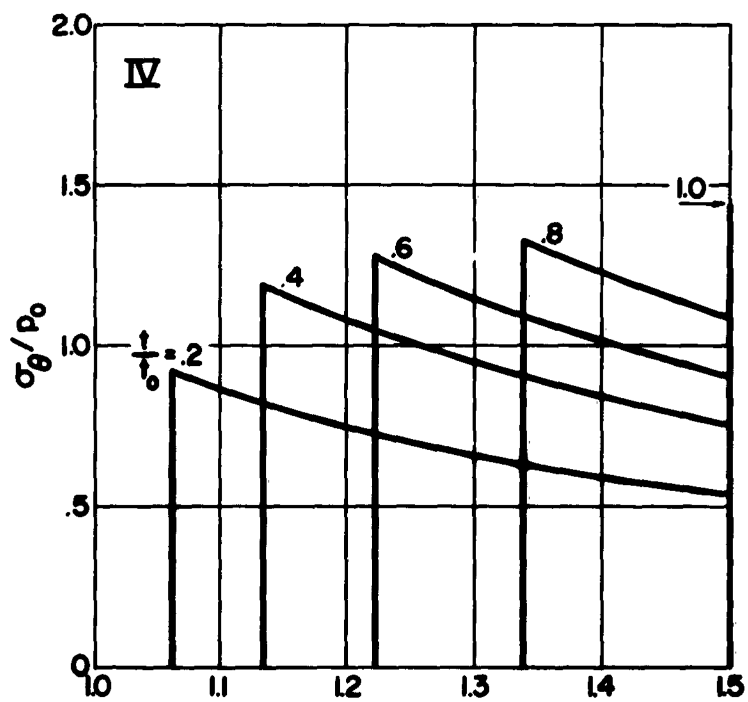

(d)

Figure 11. Space Distribution of Tangential Stresses σ_θ

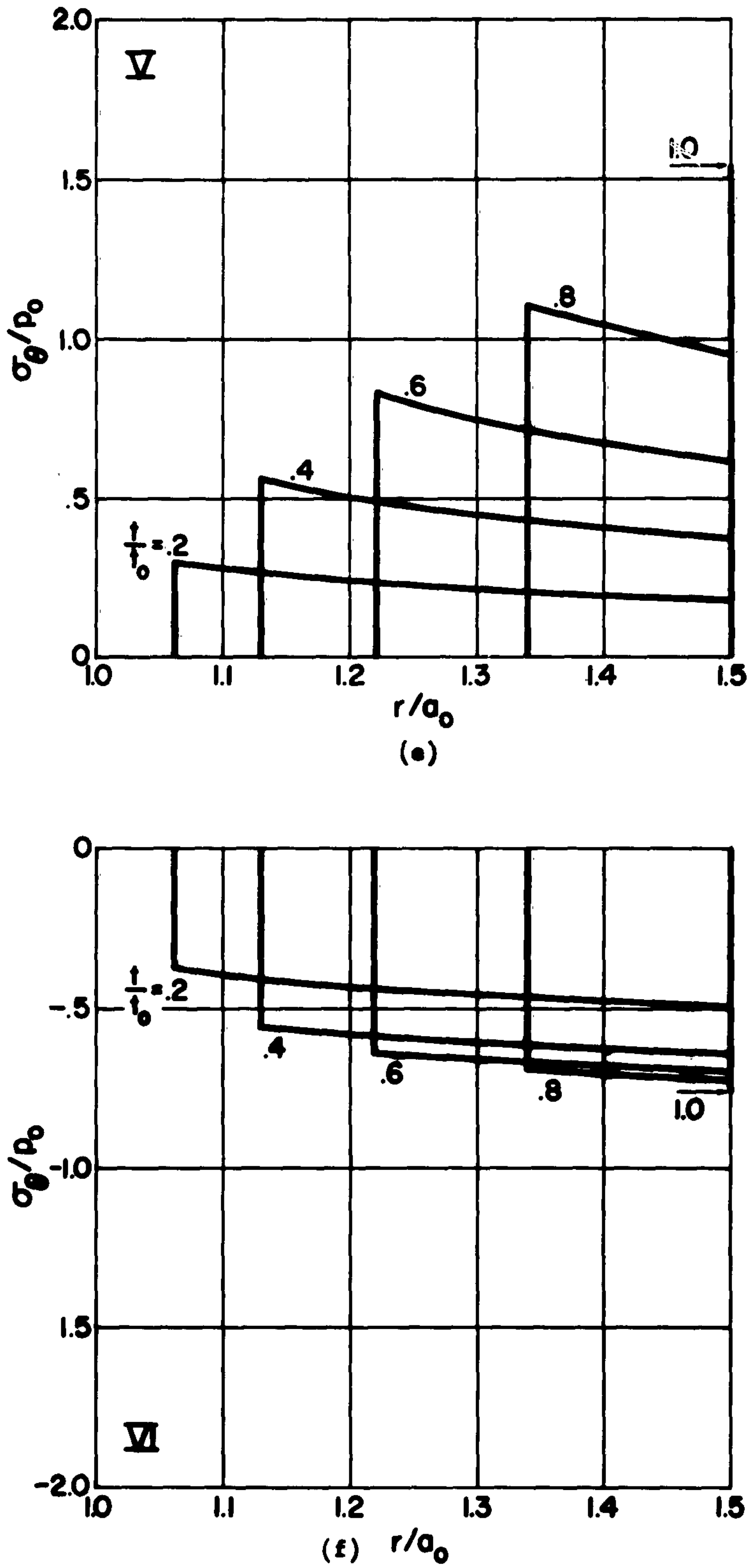

Figure 11. Space Distribution of Tangential Stresses σ_θ

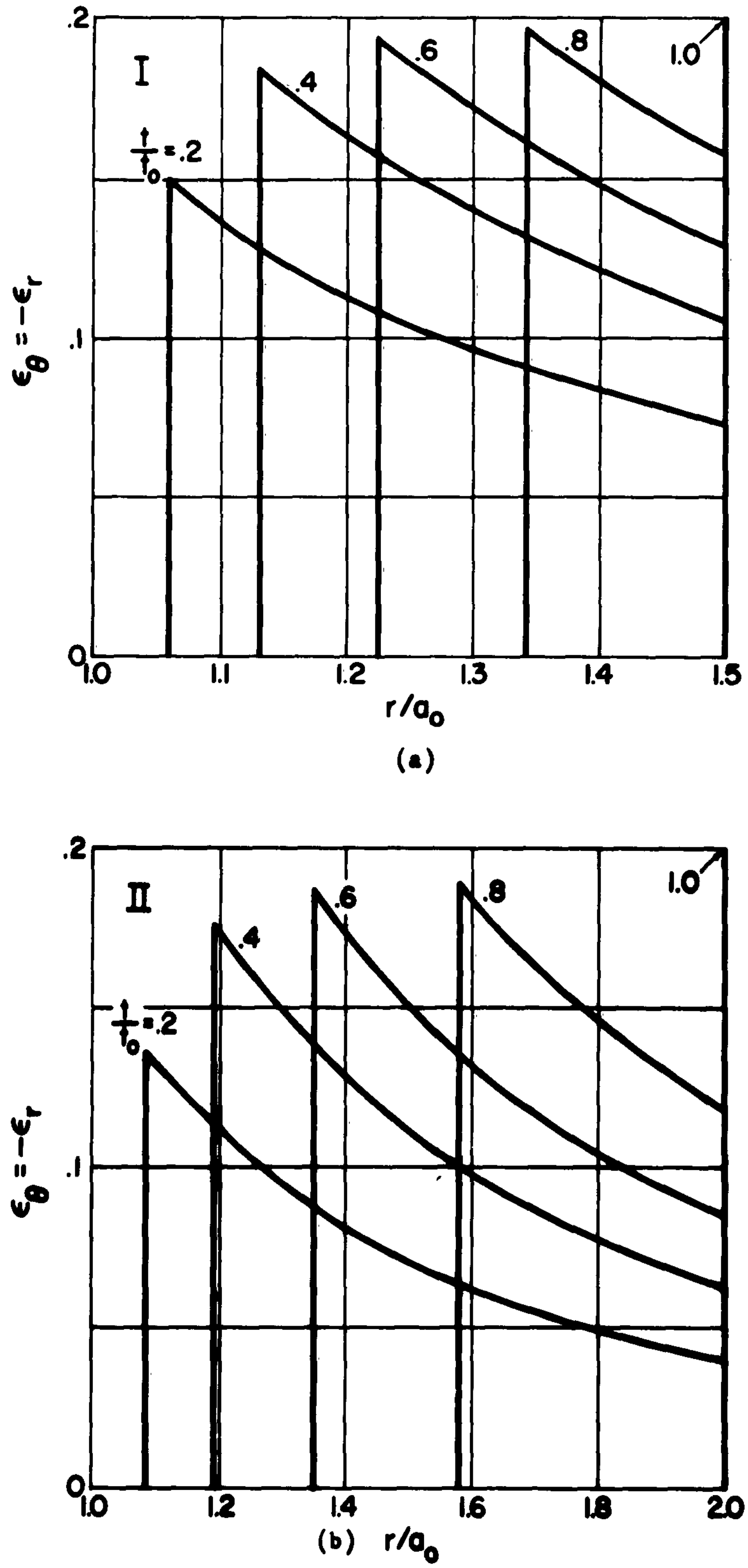

Figure 12. Space Distribution of Radial and Tangential Strains, ϵ_r and ϵ_θ

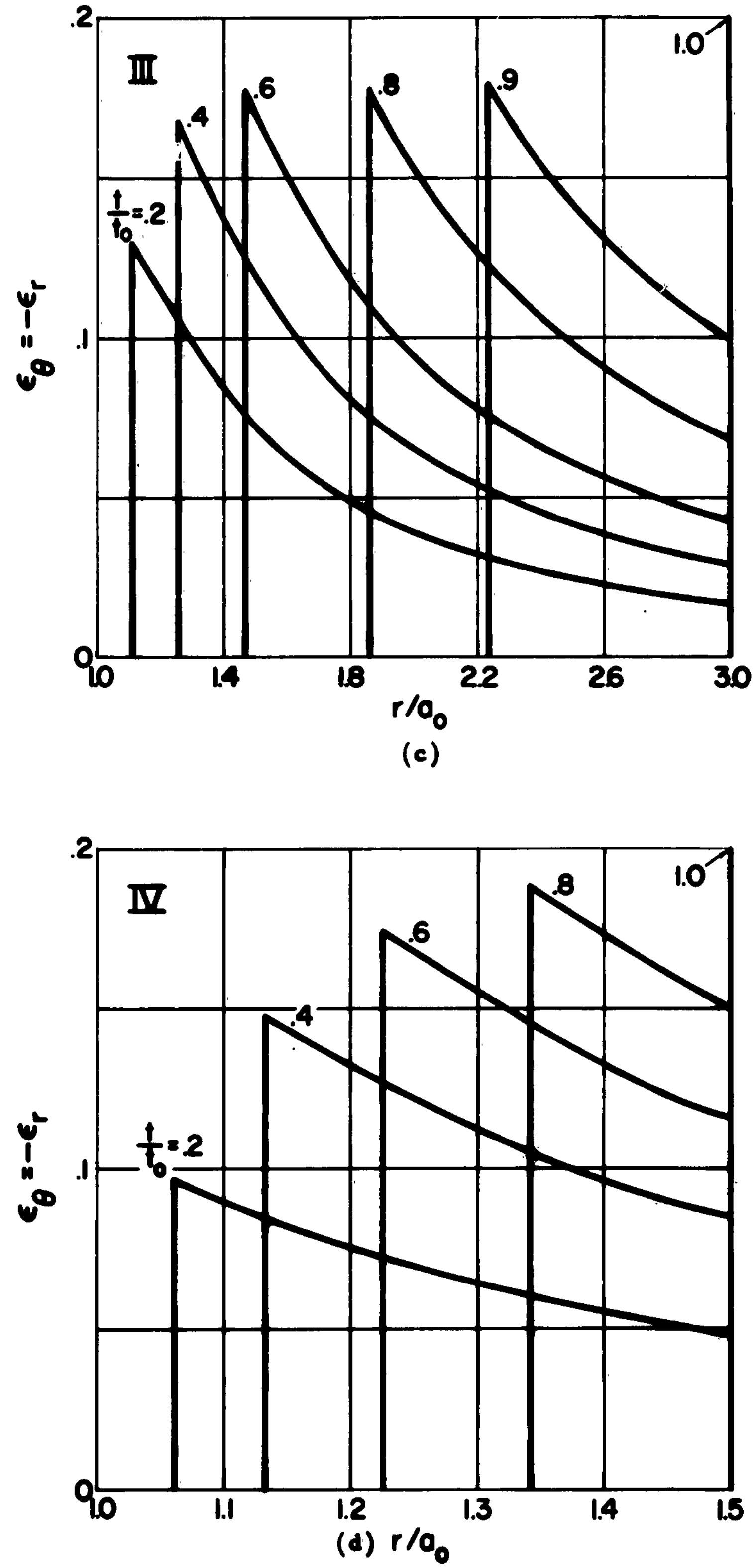

Figure 12. Space Distribution of Radial and Tangential Strains, ε_r and ε_θ

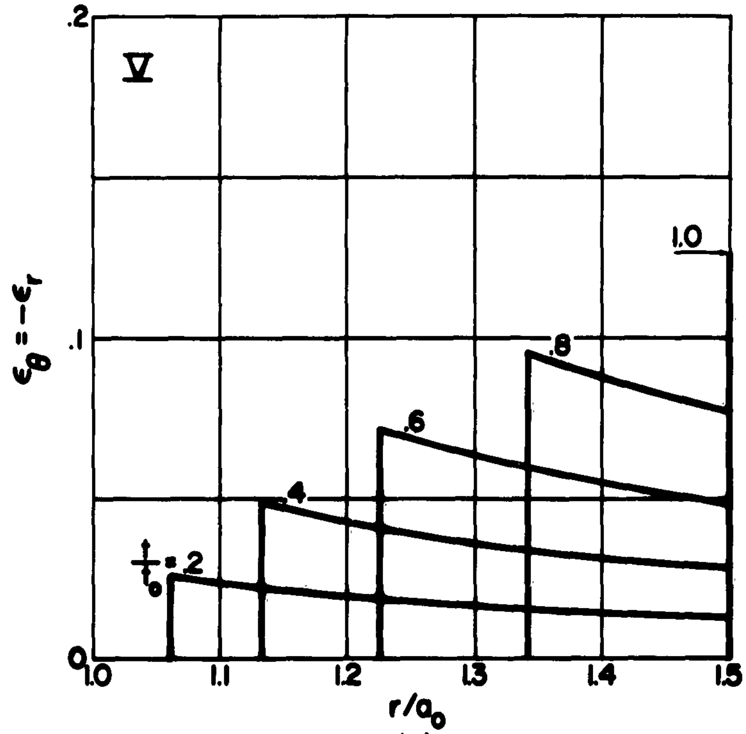

(e)

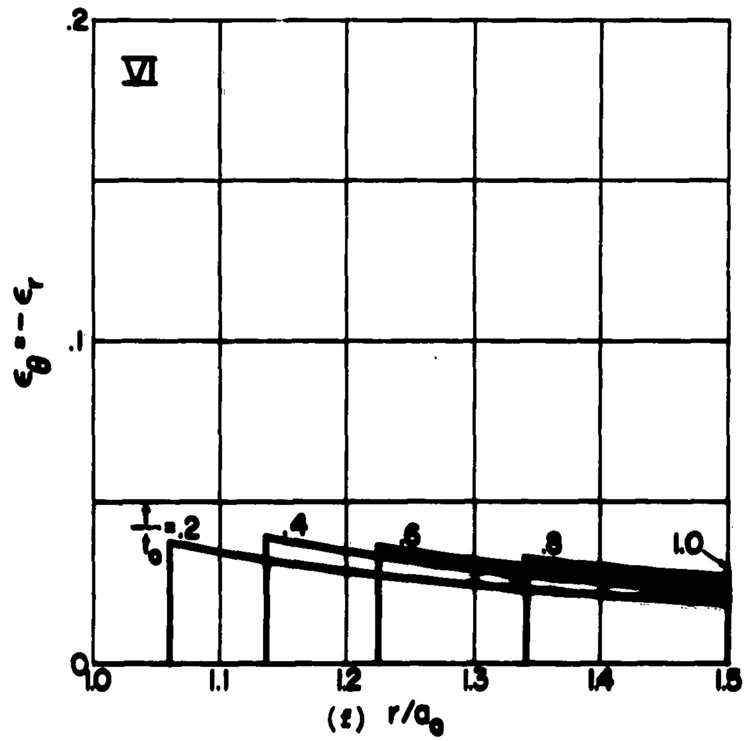

(f)

Figure 12. Space Distribution of Radial and Tangential Strains, ε_r and ε_θ

DISTRIBUTION LIST

ONR Solid Propellant Mechanics Reports

PART I - Members, POLARIS Committee

Office of Naval Research
Department of the Navy
Washington 25, D.C.
Attn: Dr. F.J. Weyl, Code 102

Applied Physics Laboratory
Johns Hopkins University
8621 Georgia Avenue
Silver Spring, Maryland
Attn: Dr. W.H. Avery

Naval Ordnance Laboratory
White Oak
Silver Spring, Maryland
Attn: Dr. D.F. Bleil

U.S. Naval Electronics Laboratory
San Diego 52, California
Attn: Dr. R.J. Christensen

Chief
Bureau of Ships
Department of the Navy
Washington 25, D.C.
Attn: Capt. W.H. Cross, Code 403

Woods Hole Oceanographic Institute
Woods Hole, Massachusetts
Attn: Dr. P.M. Fye

Chief
Bureau of Naval Weapons
Department of the Navy
Washington 25, D.C.
Attn: Dr. E.S. Lamar, CR-12

U.S. Naval Ordnance Test Station
China Lake, California
Attn: Dr. T. Phipps

Office of Naval Research
Department of the Navy
Washington 25, D.C.
Attn: Capt. W.T. Sawyer, Code 406

Chief, Bureau of Ships
Department of the Navy
Washington 25, D.C.
Attn: Dr. George Sponsler, Code 315

Director
Naval Research Laboratory
Department of the Navy
Washington 25, D.C.
Attn: Mr. P. Waterman, Code 5360

Missile and Space Division
Lockheed Aircraft Corporation
Palo Alto, California
Attn: Dr. W.F. Whitmore

Special Projects Office (SP-114)
Bureau of Naval Weapons
Department of the Navy
Washington 25, D.C.
Attn: LCDR R.H. Yerbury (Executive Secretary)

PART II - Members, SPIA Physical Properties Panel

Commander
Air Force Flight Test Center
Edwards Air Force Base, California
Attn: FTRS, D. Hart

Aberdeen Proving Group
Ballistic Research Laboratories
Aberdeen, Maryland
Attn: A.S. Elder
H.P. Gay

Redstone Arsenal
Army Rocket and Guided Missile Agency
Huntsville, Alabama
Attn: T.H. Duerr

Department of the Navy
Bureau of Naval Weapons
Washington 25, D.C.
Attn: RMMP-22, W.A. Bernett

U.S. Naval Ordnance Test Station
China Lake, California
Attn: K.H. Bischel
A. Adlcoff

U.S. Naval Propellant Plant
Indian Head, Maryland
Attn: W.J. Marciniak

Aerojet-General Corporation
P.O. Box 296
Azusa, California
Attn: K.H. Sweeny
K.W. Bills

Aerojet-General Corporation
P.O. Box 1168
Sacramento, California
Attn: J.H. Wiegand

Atlantic Research Corporation
Shirley Highway & Edsall Road
Alexandria, Virginia
Attn: M.G. DeFries

California Institute of Technology
Pasadena, California
Attn: J.P. Blatz
M.L. Williams

E.I. duPont de Nemours & Co.
Gibbstown, New Jersey
Attn: R.D. Spangler

Grand Central Rocket Company
P.O. Box 111
Redlands, California
Attn: E. Fitzgerald

Hercules Powder Company
Allegany Ballistic Laboratory
Cumberland, Maryland
Attn: J.H. Thacher

Hercules Powder Company
Bacchus Works
Magna, Utah
Attn: D.E. Nicholson

Jet Propulsion Laboratory
4800 Oak Grove Drive
Pasadena 3, California
Attn: R.F. Landel

Rocketdyne
Solid Propulsion Operations
P.O. Box 548
McGregor, Texas
Attn: S.C. Britton

Rohm and Haas Company
Redstone Arsenal Research Division
Huntsville, Alabama
Attn: A.J. Ignatowski

Space Technology Laboratory, Inc.
5730 Arbor-Vitae Street
Los Angeles 45, California
Attn: W.G. Gottenberg

Stanford Research Institute
Menlo Park, California
Attn: Dr. T.L. Smith

Thiokol Chemicals Corporation
Redstone Division
Hunstville, Alabama
Attn: M.H. Cooper

United Technology Corporation
P.O. Box 358
Sunnyvale, California
Attn: Dr. Iwanciow
Dr. F. Lavacot

Solid Propellant Information Agency
APL/JHU, 8621 Georgia Avenue
Silver Spring, Maryland
Attn: M.T. Lyons (3)

PART III - Activities and Contractors - Concerned with Propellant Mechanics

Government

Chief of Naval Research
Department of the Navy
Washington 25, D.C.
Attn: Code 439 (3)
Code 411
Commanding Officer
Cognizant ONR Branch Office

Armed Services Technical
Information Agency
Arlington Hall Station
Arlington 12, Virginia (10)

Office of Technical Services
Department of Commerce
Washington 25, D.C.

Director of Defense Research and
Engineering
The Pentagon
Washington 25, D.C.
Attn: Technical Library

Advanced Research Projects Agency
Defense Research and Engineering
The Pentagon
Washington 25, D.C.
Attn: A.M. Rubenstein

Director, Special Projects
Department of the Navy
Washington 25, D.C.
Attn: SP001 (Dr. J.P. Craven)
SP271 (LCDR R.L. McArthy)

Chief, Bureau of Naval Weapons
Department of the Navy
Washington 25, D.C.
Attn: RRRE-6 (Dr. C. Boyars)
RMMP-2 (Dr. O.H. Johnson)
RMMP-11 (Mr. I. Silver

Commander
Air Force Flight Test Center
Edwards Air Force Base, California
Attn: FTRS

Commander
Ogden Air Material Area
Hill Air Force Base, Utah
Attn: OOMQCC, H.A. Matis

Commander
Air Force Office of Scientific Research
Washington 25, D.C.
Attn: Mechanics Division

Commanding General
Aberdeen Proving Ground
Maryland
Attn: Ballistic Research Labs.
ORDBG-BLI

Commander
Army Rocket and Guided Missile Agency
Redstone Arsenal, Alabama
Attn: Technical Library
ORDXR-OTL
ORDAB-HSI

Department of the Army
Office, Chief of Ordnance
Washington 25, D.C.
Attn: ORDTB, J.A. Chalmers

Director
Plastics Tech. Eval. Center
Picatinny Arsenal
Dover, New Jersey

U.S. Army Research Office
2127 Myrtle Drive
Duke Station
Durham, North Carolina
Attn: Div. of Engineering Sciences

Chief of Naval Operations
Department of the Navy
Washington 25, D.C.
Attn: Op 07T
Op 03EG

Quality Evaluation Laboratory
Naval Ammunition Depot
Concord, California
Attn: D.R. Smathers

U.S. Naval Ordnance Laboratory
Non Metallic Materials Division
Silver Spring, Maryland
Attn: H.A. Perry, Jr.

U.S. Naval Ordnance Test Station
China Lake, California
Attn: J.T. Bartling

U.S. Naval Propellant Plant
Indian Head, Maryland
Attn: J. Browning
L. Papier (L)

Office of Naval Research
Branch Office
495 Summer Street
Boston 10, Massachusetts
Attn: Dr. J.H. Faull, Jr.

National Aeronautics & Space Adm.
1570 H Street, N.W.
Washington 25, D. C.
Attn; Chief, Div. of Research Information

Contractors

Atlantic Research, Inc.
Shirley Highway and Edsall Road
Alexandria, Virginia
Attn: M.G. DeFries

Battelle Memorial Institute
505 King Avenue
Columbus 1, Ohio
Attn: J.Harry Jackson

Brown University
Division of Applied Mathematics
Providence 12, Rhode Island
Attn: Prof. E.H. Lee
Prof. R.S. Rivlin

University of California
College of Engineering
Berkeley 4, California
Attn: Prof. Paul M.Naghdi

Catholic University of America
Department of Civil Engineering
620 Michigan Avenue, N.E.
Washington, D.C.
Attn: Prof. A.J. Durelli

Columbia University
Department of Civil Engineering
Amsterdam Avenue & 120th Street
New York 27, New York
Attn: Prof.A.M. Freudenthal

Materials Technology, Inc.
11 Leon Street
Boston 15, Massachusetts
Attn: Dr. R.G. Cheatham

New York University
Depart. of Aeronautical Engineering
University Heights
New York 53, New York
Attn: Prof. H. Becker

University of Pennsylvania
Graduate Division of Engineering Mechanics
Philadelphia 4, Pennsylvania
Attn: Prof. Z. Hashin

Polytechnic Institute of Brooklyn
333 Jay Street
Brooklyn 1, New York
Attn: Prof. F. Romano
Prof. J. Klosner
Prof. F. Ullman

Southwest Research Institute
8500 Culebra Road
San Antonio 6, Texas
Attn: Dr. R.C. DeHart

Central Laboratory T. N. O.
134 Julianalaan
Delft, Holland
Attn: Dr. F. Schwarzl

Aerojet-General Corporation
Solid Rocket Plant
Sacramento, California
Attn: Dr. W.O. Wetmore (2)

Aerojet-General Corporation
P.O. Box 1168
Sacramento, California
Attn: A. Fraser
Dr. Zickel

Amcel Propulsion, Inc.
Box 3049
Asheville, North Carolina
Attn: R.N. Lowrey

American Cyanamid Company
1937 West Main Street
Stamford, Connecticut
Attn: Dr. V. Wystrach

University of California
Berkeley, California
Attn: Dr. K.S. Pister

Catholic University of America
Department of Civil Engineering
Washington, D.C.
Attn: J. Baltrukonis

University of Florida
College of Engineering
Gainesville, Florida
Attn: J. Griffith

University of Illinois
Department of Aero Engineering
Urbana, Illinois
Attn: Dr. H.H. Hilton

E.I. duPont de Nemours and Co.
Gibbstown, New Jersey
Attn: R.D. Spangler

Grand Central Rocket Company
P.O. Box 111
Redlands, California
Attn: A.T. Camp

Hercules Powder Company
Allegany Ballistics Laboratory
Cumberland, Maryland
Attn: Dr. R. Steinberger (2)

Jet Propulsion Laboratory
4800 Oak Grove Drive
Pasadena 3, California
Attn: G. Lewis

Lockheed Missile & Space Company
1122 Jagels Road
Sunnyvale, California
Attn: E. Luken (2)

North American Aviation
Rocketdyne Division
6633 Canoga Avenue
Canoga Park, California
Attn: F. Cramer

Rohm & Haas Company
Redstone Arsenal Research Division
Huntsville, Alabama
Attn: H. Shuey

Thiokol Chemical Corporation
Redstone Division
Huntsville, Alabama
Attn: Technical Director
J. Wise

PART IV - Activities and contractors concerned with other aspects of Elastomer Mechanics

Government

Commanding Officer
Office of Naval Research
Branch Office
John Crerar Library Building
86 E. Randolph Street
Chicago 11, Illinois

Commanding Officer
Office of Naval Research
Branch Office
346 Broadway
New York 13, New York

Commanding Officer
Office of Naval Research
Branch Office
1030 E. Green Street
Pasadena, California

Commanding Officer
Office of Naval Research
Branch Office
1000 Geary Street
San Francisco, California

Commanding Officer
Office of Naval Research
Branch Office
Navy 100, Fleet Post Office
Box 39 FPO
New York, New York (5)

Director
Naval Research Laboratory
Washington 25, D.C.
Attn: Tech. Info. Officer (6)
Code 6200
Code 6210

Chief, Bureau of Ships
Department of the Navy
Washington 25, D.C.
Attn: Code 335

Professor R.L. Bisplinghoff
Department of Aeronautical Engineering
Massachusetts Institute of Technology
Cambridge 39, Massachusetts

Chief, Bureau of Yards & Docks
Department of the Navy
Washington 25, D.C.
Attn: Code 70

Commanding Officer & Director
David Taylor Model Basin
Washington 7, D.C.
Attn: Code 700

Director
Materials Laboratory
New York Naval Shipyard
Brooklyn 1, New York

Officer-in-Charge
Naval Civil Engineering Research
and Evaluation Laboratory
U.S. Naval Construction Battalion
Center
Port Hueneme, California

Commander
U.S. Naval Proving Ground
Dahlgren, Virginia

Commanding Officer & Director
U.S. Naval Engineering Experiment
Station
Annapolis, Maryland

Superintendent
U.S. Naval Postgraduate School
Monterey, California

National Sciences Foundation
1520 H Street, N.W.
Washington, D.C.
Attn: Engineering Sci. Div.

Professor H.H. Bleich
Department of Civil Engineering
Columbia University
Amsterdam Avenue & 120th Street
New York 27, New York

Professor B.A. Boley
Department of Civil Engineering
Columbia University
Amsterdam Avenue & 120th Street
New York 27, New York

Professor B. Budiansky
Department of Mechanical Engineering
School of Applied Sciences
Harvard University
Cambridge 38, Massachusetts

Professor G. F. Carrier
Pierce Hall
Harvard University
Cambridge 38, Massachusetts

Professor D.C. Drucker
Division of Engineering
Brown University
Providence 12, Rhode Island

Professor J. Ericksen
Mechanical Engineering Department
Johns Hopkins University
Baltimore 18, Maryland

Professor A.C. Eringen
Department of Aeronautical Engineering
Purdue University
Lafayette, Indiana

Mr. Martin Goland, President
Southwest Research Institute
8500 Culebra Road
San Antonio 6, Texas

Professor J.N. Goodier
Department of Mechanical Engineering
Stanford University
Stanford, California

Professor P.G. Hodge
Department of Mechanics
Illinois Institute of Technology
Chicago 16, Illinois

Professor N.J. Hoff, Head
Division of Aeronautical Engineering
Stanford University
Stanford, California

Professor J. Kempner
Dept. of Aeronautical Engineering
and Applied Mechanics
Polytechnic Institute of Brooklyn
333 Jay Street
Brooklyn, New York

Professor R.D. Mindlin
Dept. of Civil Engineering
Columbia University
Amsterdam Avenue & 120th Street
New York 27, New York

Professor William A. Nash
Dept. of Engineering Mechanics
University of Florida
Gainesville, Florida

Professor N.M. Newmark, Head
Dept. of Civil Engineering
University of Illinois
Urbana, Illinois

Professor E. Reiss
Institute of Mathematical Sciences
New York University
25 Waverly Place
New York 3, New York

Professor W. Prager, Chairman
Physical Sciences Council
Brown University
Providence 12, Rhode Island

Professor E. Reissner
Dept. of Mathematics
Massachusetts Institute of Technology
Cambridge 39, Massachusetts

Professor Bernard W. Shaffer
Dept. of Mechanical Engineering
New York University
University Heights
New York 53, New York

Professor Eli Sternberg
Dept. of Mechanics
Brown University
Providence 12, Rhode Island

Professor A.S. Velestos
Dept. of Civil Engineering
University of Illinois
Urbana, Illinois